Nov 7th, 12:00 AM - Nov 8th, 12:00 AM

Cold-Formed Ferritic Stainless Steel Tubular Sections under End-One-Flange Loading Condition

Hai-Ting Li

Benjamin Young

Wei-Wen Yu International Specialty Conference on Cold-Formed Steel Structures
St. Louis, Missouri, U.S.A., November 7 & 8, 2018

Cold-Formed Ferritic Stainless Steel Tubular Sections under End-One-Flange Loading Condition

Hai-Ting Li[1] and Ben Young[2]

Abstract

This paper presents experimental and numerical investigations of cold-formed ferritic stainless steel tubular sections under End-One-Flange (EOF) loading condition. A series of web crippling tests was conducted on cold-formed square and rectangular hollow sections of ferritic stainless steel grade EN 1.4003. The web crippling test results were used for the verification of the finite element (FE) model. Upon verification, a parametric study was performed thereafter. The codified web crippling design provisions in American, Australian/New Zealand and European standards for stainless steel structures were assessed. Improved web crippling design rules are proposed for cold-formed ferritic stainless steel tubular sections under EOF loading condition through modifying the design rules of the North American Specification and Direct Strength Method. It is shown that the modified web crippling design rules are able to provide accurate and reliable predictions.

Introduction

Cold-formed stainless steel square hollow sections (SHS) and rectangular hollow sections (RHS) are becoming increasingly attractive in engineering applications due to their favorable physical and mechanical characteristics such as aesthetic appearance, recyclability, durability, high torsional stiffness and so forth. Under local transverse bearing forces, the webs of cold-formed stainless steel SHS and RHS may cripple and, therefore, web crippling check is crucial in the design of such SHS and RHS structural members. Currently, web crippling provisions are available in the American Specification (ASCE, 2002), Australian/New Zealand Standard (AS/NZS, 2001) and European Code (EC3, 2015) for stainless steel

[1] Postdoctoral Fellow, Department of Civil Engineering, The University of Hong Kong, Pokfulam Road, Hong Kong, China.
[2] Professor, Department of Civil Engineering, The University of Hong Kong, Pokfulam Road, Hong Kong, China.

structures. However, it should be noted that the codified web crippling design provisions of stainless steel sections in the aforementioned codes of practice are adopted from provisions of carbon steel sections. This is mainly due to the lack of research conducted on stainless steel sections undergoing web crippling.

Ferritic stainless steels, having relatively lower initial material cost, may offer more viable alternatives for structural applications than other stainless steel grades (Afshan & Gardner, 2013; Tao & Rasmussen, 2016). Recently, a research project entitled Structural Applications of Ferritic Stainless Steels (SAFSS) was conducted in Europe to increase the use of ferritic stainless steels in construction. In the SAFSS project, web crippling tests under the End-One-Flange (EOF) and Interior-One-Flange (IOF) loading conditions were conducted on ferritic stainless steel SHS (2 tests) and hat sections of grade EN 1.4509 (Talja & Hradil, 2011). A numerical investigation on ferritic stainless steel hollow and hat sections under EOF and IOF loading conditions were performed by Bock et al. (2013), and design rules, which considered strain hardening effects, were proposed based on the design provisions in the EC3. Moreover, Islam & Young (2012) investigated carbon fiber reinforced polymer (CFRP) strengthening for ferritic stainless steel SHS and RHS subjected to web crippling. To date, however, investigations on cold-formed ferritic stainless steel SHS and RHS undergoing web crippling are still rather limited.

In this paper, experimental and numerical investigations were carried out to study the web crippling behavior of cold-formed ferritic stainless steel SHS and RHS under the EOF loading condition as specified in the ASCE (2002) and AS/NZS (2001). A series of web crippling tests was first conducted and a finite element (FE) model was developed thereafter. Upon verification of the FE model, a parametric study was performed using the verified FE model to expand the database. The codified web crippling provisions in the ASCE (2002), AS/NZS (2001) and EC3 (2015) were evaluated. Improved design rules are proposed for cold-formed ferritic stainless steel SHS and RHS under the EOF loading condition by modifying the design rules of the North American Specification (NAS, 2016) as well as Direct Strength Method.

Experimental Investigation

A series of web crippling tests was conducted on cold-formed SHS and RHS of ferritic stainless steel grade EN 1.4003. The web heights (H), flange widths (B), thicknesses (t), inner corner radii (r) and outer corner radii (R) of the cross-sections as well as the member lengths (L) of the test specimens were measured and reported in Table 1. The measured H ranged from 50.1 to 100.2 mm, measured B ranged from 40.0 to 80.0 mm and measured t ranged from 1.925 to 3.829 mm.

The measured r and R ranged from 2.6 to 4.0 mm and 5.4 to 8.2 mm, respectively. The measured web slenderness ratios, h/t, ranged from 9.0 to 45.9, where h is the depth of the web flat portion. The specimen lengths L were determined in accordance with the ASCE (2002) and AS/NZS (2001), as indicated in Figure 1.

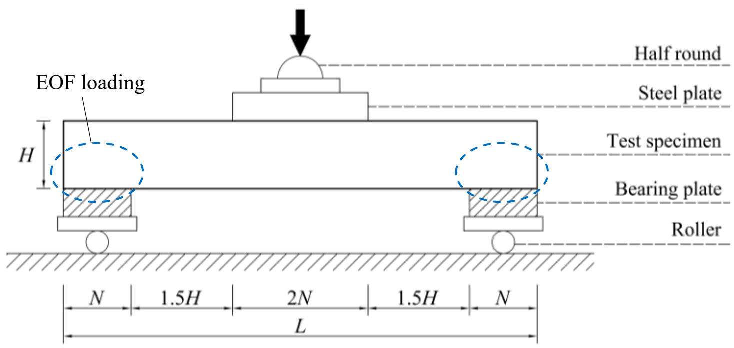

Figure 1: End-One-Flange loading condition

Table 1: Measured specimen dimensions and experimental web crippling strengths per web

Specimen	H (mm)	B (mm)	t (mm)	r (mm)	R (mm)	L (mm)	P_{Exp} (kN)
EOF-50×50×4N50	50.1	50.2	3.826	4.0	8.2	350	31.8*
EOF-50×50×4N30	50.1	50.2	3.829	4.0	8.2	269	34.6*
EOF-80×80×3N90	80.0	80.0	2.807	3.0	5.8	600	36.3*
EOF-80×80×3N50	80.0	80.0	2.803	3.0	5.8	441	37.8
EOF-60×40×3N50	60.0	40.0	2.734	3.1	5.9	381	21.7*
EOF-60×40×3N30	60.0	40.1	2.716	3.1	5.9	300	22.4
EOF-60×40×3N30-R[†]	60.0	40.0	2.716	3.1	5.9	301	22.3
EOF-100×40×2N50	99.8	40.3	1.931	3.8	5.7	499	12.1
EOF-100×40×2N30	99.8	40.2	1.925	3.8	5.7	420	9.0
EOF-100×50×3N50	100.2	50.0	2.796	2.6	5.4	500	32.9
EOF-100×50×3N30	100.2	49.9	2.792	2.6	5.4	419	23.9

Note: *Specimen failed near mid-span; [†]Repeated test.

Longitudinal tensile flat and corner coupon tests were conducted to obtain the material properties of the SHS and RHS. In addition to the tensile coupon tests, transverse compressive flat coupon tests were also carried out. The material properties obtained from the tensile flat, compressive flat and tensile corner coupon tests are tabulated in Table 2. The test specimens were from the same batch of ferritic stainless steel tubes as described in Li & Young (2017a), where detailed descriptions of the coupon tests can be found.

Table 2: Material properties obtained from coupon tests

Section ($H \times B \times t$)	Tensile Flat		Compressive flat		Tensile corner	
	E^{T} (GPa)	$\sigma_{0.2}^{T}$ (MPa)	E^{C} (GPa)	$\sigma_{0.2}^{C}$ (MPa)	E_{c} (GPa)	$\sigma_{0.2,c}$ (MPa)
50×50×4^	196.4	459	217.8	527	190.7	557
80×80×3	195.0	417	215.1	461	196.3	552
60×40×3^	204.4	401	228.6	507	200.5	531
100×40×2^	200.5	426	202.9	423	209.8	544
100×50×3^	198.1	428	206.3	463	189.2	519

Note: ^ Conducted by Li & Young (2017a).

The web crippling tests were conducted under the EOF loading condition that specified in the ASCE (2002) and AS/NZS (2001), as illustrated in Figure 1, where the locations of the failure in the member are shown by blue color circles in the diagram. The web crippling test setup can be found in Figure 2. The loading or reaction forces were applied to the ferritic stainless steel SHS and RHS through high strength steel bearing plates. Two bearing plates supported by two rollers were positioned at both ends of the EOF specimens to provide symmetric loading. A steel plate of twice the bearing plate width was positioned at the mid-span of the EOF specimen, and a half round was employed to transfer the applied loads. The bearing plates were designed to act across the full-flange widths of the SHS and RHS. To prevent failure near mid-span of the specimen, a wooden block was inserted inside the specimen and steel stiffening plates of twice the width of the bearing plate were also clamped at mid-span of the specimen on both sides. It should be noted that all flanges of the specimens were not fastened to the bearing plates during testing. A servo-controlled hydraulic testing machine was employed to apply compressive forces to the test specimens and displacement control was employed to drive the hydraulic actuator at a constant speed of 0.3 mm/min. Vertical web deformations of the SHS and RHS specimens were measured between the bearing plates and the top flange of the specimens near the corners by the average readings of two calibrated linear variable displacement transducers (LVDTs) at one of the ends that failure occurred. In addition, lateral web deformations were also measured by the average readings of two LVDTs that rigidly connected with flat plastic plates and, therefore, the maximum lateral web deformations of the specimens can be captured (Li & Young, 2017b).

The experimental web crippling ultimate strengths per web P_{Exp} are reported in Table 1. Typical experimental web crippling failure mode can be found in Figure

2. It is noteworthy that specimens EOF-50×50×4N50, EOF-50×50×4N30, EOF-80×80×3N90 and EOF-60×40×3N50 failed near the mid-span instead of web crippling failure. Hence, the test results of these four specimens were not compared with the nominal strengths calculated from design provisions at a later stage.

Numerical Modelling Approach

Finite Element Model

In conjunction with the experimental investigation, a finite element (FE) model was developed to replicate the web crippling tests using the FE analysis package ABAQUS (2012). The FE model was developed based on measured test specimen geometries. The material nonlinearity was incorporated into the FE model based on the measured stress-strain data obtained from the coupon tests. The webs of the cold-formed ferritic stainless steel SHS and RHS were under compressive stresses acting along the transverse direction during testing. Therefore, in the FE model, the measured stress-strain data obtained from transverse compressive flat coupon tests were used for the webs of the SHS and RHS, whilst the measured stress-strain data from longitudinal tensile flat coupon tests were employed for the flanges. In addition, the measured stress-strain data of longitudinal tensile corner coupons were applied to the corner portions of the SHS and RHS with an extension of $2t$ to the adjacent flat regions.

The shell element S4R was used to simulate the ferritic stainless steel SHS and RHS specimens. The applied meshes in the flat portions of the SHS and RHS ranged from 4×4 to 8×8 mm, which depends on the cross-section sizes, and finer meshes were used at the round corners. The steel bearing plates were modeled by means of discrete rigid 3D solid elements. The interfaces between the bearing plates and the specimens were modeled using the surface-to-surface discretization contact method. The "hard" contact was adopted and the friction penalty contact with a friction coefficient of 0.4 was applied. The boundary conditions were modeled in accordance with the tests. The loads were applied to the ferritic stainless steel SHS and RHS specimens by specifying axial displacements to the reference points of bearing plates, which was identical to the tests using displacement control.

Verification of Finite Element Model

The developed FE model was verified against the web crippling test results. The experimental web crippling strengths, failure modes and load-deformation curves obtained from the 7 tests, which failed by web crippling, were compared with those derived from the FE analyses. The web crippling strengths per web P_{FEA} derived from the FE analyses are reported in Table 3. The mean value of the P_{Exp}/P_{FEA} was 1.02 with the coefficient of variation (COV) of 0.057. Typical numerical failure mode was compared with the corresponding experimental failure mode, as shown in Figure 2. Typical numerical load-lateral web deformation curve was also compared with that obtained experimentally in Figure 3. It can be observed that the FE model was capable of replicating the experimental ultimate strength, failure mode and load-deformation behavior.

Table 3: Comparison of test strengths with finite element results

Specimen	h/t	P_{Exp} (kN)	P_{FEA} (kN)	P_{Exp}/P_{FEA}
EOF-80×80×3N50	24.4	37.8	34.0	1.11
EOF-60×40×3N30	17.8	22.4	22.0	1.02
EOF-60×40×3N30-R†	17.8	22.3	22.0	1.01
EOF-100×40×2N50	45.7	12.1	12.4	0.97
EOF-100×40×2N30	45.9	9.0	9.6	0.94
EOF-100×50×3N50	32.0	32.9	31.6	1.04
EOF-100×50×3N30	32.0	23.9	22.5	1.06
			Mean	1.02
			COV	0.057

Note: †Repeated test.

(a) Experimental failure mode

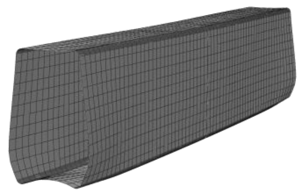

(b) Numerical failure mode

Figure 2: Experimental and numerical failure modes of specimen EOF-100×50×3N50

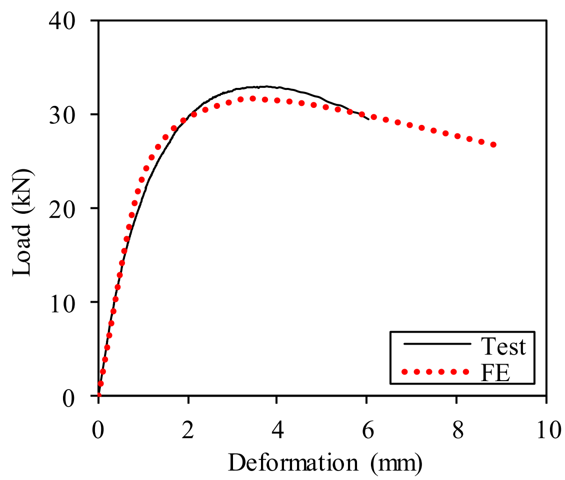

Figure 3: Load-lateral web deformation curves of specimen EOF-100×50×3N50

Parametric Study

Upon verification of the FE model, a parametric study was carried out using the verified model to generate further numerical date over a wider range of key web crippling parameters (e.g., web slenderness ratio, bearing length to thickness ratio and bearing length to web flat portion ratio). Various cross-sections including 8 SHS and 12 RHS were investigated in the parametric study herein. The cross-sectional dimensions (H×B×t) of the SHS ranged from 70×70×1.5 to 200×200×4, and the RHS ranged from 80×140×1.5 to 300×200×5. Two bearing lengths (N) were employed for each cross-section and the N were either taken as B or 0.5B. In the parametric study, the specimen lengths were determined in accordance with the ASCE (2002) and AS/NZS (2001), and the material modeling was based on the measured stress-strain data obtained from the coupon tests of the section

80×80×3. The parametric study specimens had the web slenderness ratios h/t ranged from 10 to 121 and bearing length to thickness ratios N/t ranged from 7 to 100. A total of 40 results were generated in the parametric study. It should be noted that, 6 specimens failed near the mid-span instead of web crippling failure. Similar observations were also found in the test program. The test and FE strengths of these EOF specimens were not used to compare with the nominal strengths calculated from design rules.

Codified Web Crippling Design Provisions

American Specification and Australian/New Zealand Standard

Web crippling provisions for cold-formed stainless steel sections are available in Clause 3.3.4 of the ASCE (2002). The AS/NZS (2001) provides provisions for predicting the web crippling strength, known as the bearing capacity, for cold-formed stainless steel sections. The AS/NZS (2001) has adopted the web rippling provisions from the American Specification. Therefore, the nominal strengths per web predicted by the AS/NZS (2001) and ASCE (2002) are identical. Note that for sections with two or more webs, such as SHS and RHS, the nominal web crippling strength should be computed for each individual web.

European Code

The web crippling provisions in the EC3 Part 1-4 (EC3, 2015) for stainless steel structures refer to the EC3 Part 1-3 (EC3, 2006) for cold-formed carbon steel structures. The codified provisions for cross-sections with two or more webs are specified in Clause 6.1.7.3 of the EC3 (2006). According to Figure 6.9 of the EC3 (2006), the EOF loading condition that specified in the ASCE (2002) and AS/NZS (2001) belongs to Category 1 in the EC3 (2006). It is noteworthy that the EC3 (2006) do not have explicit web crippling coefficient for tubular sections. In this study, the web crippling coefficient of 0.057 was employed.

Comparison of Web Crippling Strengths with Codified Design Predictions

The codified web crippling design provisions were assessed. A data pool of 46 cold-formed ferritic stainless steel SHS and RHS specimens was used, including the test and FE data obtained in the present study and the available data reported in the literature (Talja & Hradil, 2011; Islam & Young, 2012). The web crippling strengths per web were compared with the nominal strengths per web predicted by the ASCE (2002), AS/NZS (2001) and EC3 (2015). The material properties obtained from the longitudinal tensile flat coupon tests and transverse compressive flat coupon tests were used to calculate the nominal strengths per web P^{T} and P^{C} for the aforementioned design provisions, respectively. The comparison of the test and FE strengths per web P_{u} with the P^{T} and P^{C} are shown in Table 4.

The reliability levels of the codified web crippling design provisions in the ASCE (2002) and EC3 (2015) were assessed. In addition, the two modified design rules proposed in this paper were also evaluated. The reliability calculations performed herein conformed to the principles detailed in the Commentary of the ASCE (2002). In this study, the design provisions are considered to be reliable if the calculated reliability index (β) is greater than or equal to 2.5. The resistance factors (ϕ) for members undergoing web crippling as recommended by the ASCE (2002) and EC3 (2015) as well as suggested for the modified design rules are tabulated in Table 4. The load combination of 1.2DL+1.6LL (DL = Dead Load and LL = Live Load) was used for the ASCE (2002) and the two modified design rules, while the load combination of 1.35DL+1.5LL was employed for the EC3 (2015). The dead-to-live load ratio of 1/5 was used. The mean values and COVs of the test and FE results to design prediction ratios are shown in Table 4. A correction factor C_{P} calculated in accordance with Eq. K2.1.1-4 of the NAS (2016) was used to account for the influence of a limited number of data. The calculated β values are reported in Table 4.

Overall, the nominal strengths per web predicted by the ASCE (2002) and AS/NZS (2001) were found to be conservative and reliable for the EOF specimens. The mean values of the test and FE-to-predicted strength ratios $P_{\mathrm{u}}/P^{\mathrm{T}}_{\mathrm{ASCE}}$ and $P_{\mathrm{u}}/P^{\mathrm{C}}_{\mathrm{ASCE}}$ were 1.14 and 1.13 with the COVs of 0.142 and 0.148, and the corresponding β values of 3.57 and 3.51, respectively. For the EC3 (2015), the codified web crippling provision was overly conservative for the cold-formed ferritic stainless SHS and RHS under the EOF loading condition. The mean values of the $P_{\mathrm{u}}/P^{\mathrm{T}}_{\mathrm{EC3}}$ and $P_{\mathrm{u}}/P^{\mathrm{C}}_{\mathrm{EC3}}$ was 3.36 and 3.13 with the COVs of 0.237 and 0.231, respectively. The EC3 comparison results revealed a relatively high level of scattering, which may have been due to the design provisions in the EC3 (2006) used a constant bearing length of 10 mm for the EOF loading condition (Category 1), despite the fact that the SHS and RHS were loaded through various bearing lengths. In this study, the P_{u} were also compared with the $P^{\mathrm{T}}_{\mathrm{EC3\#}}$ and $P^{\mathrm{C}}_{\mathrm{EC3\#}}$ that calculated through the actual bearing lengths, as shown in Table 4. Overall, it can be observed that the EC3 (2015) provided conservative and reliable predictions with a relatively low level of scattering for the EOF specimens when the actual bearing lengths were used.

Table 4: Comparison between experimental and numerical results with nominal design strengths

EOF	ASCE		EC3				NAS#		DSM	
	$\frac{P_u}{P^T_{ASCE}}$	$\frac{P_u}{P^C_{ASCE}}$	$\frac{P_u}{P^T_{EC3}}$	$\frac{P_u}{P^C_{EC3}}$	$\frac{P_u}{P^T_{EC3\#}}$	$\frac{P_u}{P^C_{EC3\#}}$	$\frac{P_u}{P^T_{NAS\#}}$	$\frac{P_u}{P^C_{NAS\#}}$	$\frac{P_u}{P^T_{DSM}}$	$\frac{P_u}{P^C_{DSM}}$
No. of data	46	41	46	41	46	41	46	41	46	41
Mean	1.14	1.13	3.36	3.13	2.04	1.85	1.08	0.97	1.06	0.99
COV	0.142	0.148	0.237	0.231	0.155	0.161	0.070	0.081	0.064	0.064
ϕ	0.70	0.70	0.91	0.91	0.91	0.91	0.85	0.85	0.85	0.85
β	3.57	3.51	5.21	5.06	4.48	4.06	3.04	2.58	2.99	2.69

Modified Design Rules and Comparison with Web Crippling Strengths

Modified North American Specification

The North American Specification (NAS, 2016) is a specified design standard for cold-formed carbon or low-alloy steels. It should be noted that the current ASCE (2002) for cold-formed stainless steel structures adopted the web crippling provisions from the American Iron and Steel Institute (AISI) Specification for cold-formed carbon steel structures. However, the AISI Specification has been superseded by the NAS (2016). A unified equation, as shown in Eq. (1), was adopted by the NAS (2016) for web crippling check. The unified equation accommodates various cross-section geometries and loading conditions through different sets of coefficients. In this study, a new set of coefficients of the unified equation is proposed for cold-formed ferritic stainless steel SHS and RHS under the EOF loading condition. The newly proposed coefficients C, C_r, C_N and C_h are 2, 0.40, 2.15 and 0.053, respectively. The coefficients were calibrated against the test and FE data obtained in this study as well as the available data reported by Talja & Hradil (2011) and Islam & Young (2012). The validity limits of the proposed coefficients are $10 \leq h/t \leq 120$, $r/t \leq 2$, $N/t \leq 100$, $N/h \leq 1.1$ and $\theta = 90°$. A resistance factor of 0.85 is suggested to be used for limit state design.

$$P_{NAS\#} = Ct^2\sigma_{0.2}\sin\theta\left(1 - C_r\sqrt{r/t}\right)\left(1 + C_N\sqrt{N/t}\right)\left(1 - C_h\sqrt{h/t}\right) \quad (1)$$

in which, $P_{NAS\#}$ is the nominal strength per web; $\sigma_{0.2}$ is the 0.2% proof stress; C, C_r, C_N and C_h are the overall coefficient, inside bend radius coefficient, bearing length coefficient and web slenderness coefficient, respectively; θ is the web inclination angle.

The P_u were compared with the $P_{NAS\#}$ calculated from the modified NAS. The mean values of the $P_u/P^T_{NAS\#}$ and $P_u/P^C_{NAS\#}$ were 1.08 and 0.97 with the COVs of

0.070 and 0.081, respectively. The reliability indices of the modified NAS, as reported in Table 4, were greater than the target value of 2.5, indicating that the nominal strengths per web calculated from the modified NAS were reliable.

Modified Direct Strength Method

The authors previously proposed Direct Strength Method (DSM) based web crippling design rules for cold-formed ferritic stainless steel SHS and RHS under end loading (EL) and interior load (IL) conditions (Li & Young, 2017a). In this study, the DSM is modified for the cold-formed ferritic stainless steel tubular sections under the EOF loading condition that specified in the ASCE (2002) and AS/NZS (2001). The web crippling strengths per web (P_{DSM}) based on modified DSM is obtained by Eq. (2). The corresponding coefficients *a, b, n,* λ_{k} and γ for cold-formed ferritic stainless steel SHS and RHS is tabulated in Table 5.

$$P_{\mathrm{DSM}}=\begin{cases}\gamma\cdot P_{\mathrm{y}} & \lambda\le\lambda_{\mathrm{k}}\\ a\left[1-b\left(\dfrac{P_{\mathrm{cr}}}{P_{\mathrm{y}}}\right)^{n}\right]\left(\dfrac{P_{\mathrm{cr}}}{P_{\mathrm{y}}}\right)^{n}P_{\mathrm{y}} & \lambda>\lambda_{\mathrm{k}}\end{cases}\tag{2}$$

in which, $\lambda = (P_{\mathrm{y}}/P_{\mathrm{cr}})^{0.5}$ is the web crippling slenderness ratio; P_{y} is the bearing yield strength per web; and P_{cr} is the bearing buckling strength per web. The determination of the P_{y} and P_{cr} in Clause 5.13 of the AS4100 (1998) are used for the EOF loading condition herein. The P_{y} is determined as follows:

$$P_{\mathrm{y}}=\alpha_{\mathrm{p}}tN_{\mathrm{m}}\sigma_{0.2}\tag{3}$$

$$\alpha_{\mathrm{p}}=\frac{0.5}{k_{\mathrm{s}}}\left[1+\left(1-\alpha_{\mathrm{pm}}^{2}\right)\left(1+\frac{k_{\mathrm{s}}}{k_{\mathrm{v}}}-\left(1-\alpha_{\mathrm{pm}}^{2}\right)\frac{0.25}{k_{\mathrm{v}}^{2}}\right)\right]\tag{4}$$

In Eqs. (3) and (4), $N_{\mathrm{m}} = N+2.5R+0.5h$ is the mechanism length, where N is the bearing length, R is outer corner radius and h is the web flat portion; $k_{\mathrm{s}} = 2R/t-1$, $\alpha_{\mathrm{pm}} = 1/k_{\mathrm{s}}+0.5/k_{\mathrm{v}}$ and $k_{\mathrm{v}} = h/t$.

The bearing buckling strength per web P_{cr} can be determined in accordance with Clause 5.13.4 of the AS4100 (1998). The single web of SHS and RHS is treated in the same way as that of a column in compression and the geometrical slenderness ratio shall be taken as $3.8h/t$ for the EOF loading condition. The P_{cr} can be determined from the equation as follows:

$$P_{\mathrm{cr}}=\alpha_{\mathrm{c}}tN_{\mathrm{m}}\sigma_{0.2}\tag{5}$$

in which, α_c is the slenderness reduction factor that detailed in Clause 6.3.3 of the AS4100 (1998).

Comparisons of the P_u with the modified DSM curve for the SHS and RHS under the EOF loading condition are displayed in Figure 4, where the data points obtained by using the $\sigma_{0.2}^{T}$ and $\sigma_{0.2}^{C}$ are indicated by "(T)" and "(C)" in the figure legend, respectively. It is shown that the modified DSM curve aligned well with the test and FE results. The mean values of the P_u/P_{DSM}^{T} and P_u/P_{DSM}^{C} were 1.06 and 0.99 with the COVs of 0.064 and 0.064 for the EOF specimens, respectively. The modified DSM revealed the highest accuracy and lowest level of scattering among all the design rules, as indicated in Table 4. The β values of the modified DSM, as reported in Tables 4, were greater than 2.5, demonstrating that the nominal strengths calculated from the modified DSM provided reliable limit state design when calibrated with the suggested ϕ of 0.85.

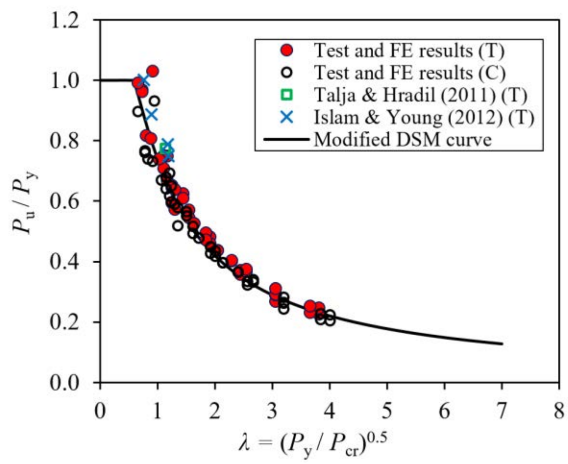

Figure 4: Comparison of test and FE results with modified DSM curve for cold-formed ferritic stainless steel SHS and RHS under EOF loading condition

Table 5: Proposed coefficients for design rules based on DSM

Load case	*a*	*b*	*n*	λ_k	γ
EOF	0.96	0.23	0.51	0.584	1.00

Note: The above coefficients apply when $10 \leq h/t \leq 120$, $r/t \leq 2$, $N/t \leq 100$, $N/h \leq 1.1$ and $\theta = 90°$.

Conclusions

The web crippling behavior of cold-formed ferritic stainless steel square and rectangular hollow sections (SHS and RHS) was investigated. A series of tests was conducted under the End-One-Flange (EOF) loading condition as specified in the American Specification (ASCE, 2002) and Australian/New Zealand Standard (AS/NZS, 2001) for cold-formed stainless steel structures. A Finite element (FE) model was developed and verified against the test results, showing the capability of replicating the experimental web crippling strength, failure mode and load-deformation history. Upon verification of the FE model, a parametric study was performed thereafter. The codified web crippling design provisions in the current ASCE (2002), AS/NZS (2001) and European Code (EC3, 2015) were assessed. Improved design rules have been proposed for cold-formed ferritic stainless steel SHS and RHS under the EOF loading condition by means of modified North American Specification (NAS, 2016) and Direct Strength Method. The reliability levels of the design rules have been evaluated. It is shown that the modified design rules can provide safe and reliable limit state design when calibrated with the suggested resistance factor of 0.85.

Acknowledgments

The authors are grateful to STALA Tube Finland for providing the test specimens. The research work described in this paper was supported by a grant from the Research Grants Council of the Hong Kong Special Administrative Region, China (Project No. HKU718612E).

Appendix. – References

ABAQUS. (2012). Abaqus/Standard user's manual volumes I-III and Abaqus CAE manual. Version 6.12. Hibbitt, Karlsson & Sorensen, Inc., Pawtucket, USA.

Afshan, S. and Gardner, L. (2013). Experimental study of cold-formed ferritic stainless steel hollow sections. Journal of Structural Engineering, 139(5): 717–728.

AS4100. (1998). Steel structures. AS 4100, Standards Australia, Sydney, Australia.

ASCE. (2002). Specification for the design of cold-formed stainless steel structural members. SEI/ASCE8-02, American Society of Civil Engineers, Reston, Virginia, USA.

AS/NZS. (2001). Cold-formed stainless steel structures. AS/NZS 4673. Standards Australia, Sydney, Australia.

Bock, M., Arrayago, I., Real, E. and Mirambell, E. (2013). Study of web crippling in ferritic stainless steel cold formed sections. Thin-Walled Structures, 69: 29–44.

EC3. (2006). Eurocode 3: Design of steel structures – Part 1-3: General rules – Supplementary rules for cold-formed members and sheeting. EN 1993-1-3, European Committee for Standardization, Brussels, Belgium.

EC3. (2015). Eurocode 3: Design of steel structures – Part 1-4: General rules – Supplementary rules for stainless steels. EN 1993-1-4:2006+A1:2015, European Committee for Standardization, Brussels, Belgium.

Islam, S.M.Z. and Young, B. (2012). Ferritic stainless steel tubular members strengthened with high modulus CFRP plate subjected to web crippling. Journal of Constructional Steel Research, 77: 107–118.

Li, H.T. and Young, B. (2017a). Cold-formed ferritic stainless steel tubular structural members subjected to concentrated bearing loads. Engineering Structures, 145: 392–405.

Li, H.T. and Young, B. (2017b). Tests of cold-formed high strength steel tubular sections undergoing web crippling. Engineering Structures, 141: 571–583.

NAS. (2016). North American Specification for the design of cold-formed steel structural members. AISI S100-16, American Iron and Steel Institute, Washington, D.C., USA.

Talja, A. and Hradil, P. (2011). SAFSS Work Package 2: Model calibration tests. Technical Research Centre of Finland (VTT), Finland.

Tao, Z. and Rasmussen, K.J.R. (2016). Stress-strain model for ferritic stainless steels. Journal of Materials in Civil Engineering, 28(2): 06015009.

Appendix. – Notation

B = Overall width of cross-section;
E^{C} = Elastic modulus obtained from compressive flat coupon test;
E^{T} = Elastic modulus obtained from tensile flat coupon test;
E_{c} = Elastic modulus obtained from tensile corner coupon test;
H = Overall depth of cross-section;
L = Specimen length;
N = Bearing length;
N_{m} = Mechanism length;
P^{C} = Nominal web crippling strength per web calculated using compressive flat material properties;
P^{T} = Nominal web crippling strength per web calculated using tensile flat material properties;
P^{C}_{ASCE} = Nominal web crippling strength per web obtained from American Specification using compressive flat material properties;

$P^{\mathrm{T}}_{\mathrm{ASCE}}$ = Nominal web crippling strength per web obtained from American Specification using tensile flat material properties;
P_{DSM} = Nominal web crippling strength per web obtained from the modified direct strength method;
$P^{\mathrm{C}}_{\mathrm{DSM}}$ = Nominal web crippling strength per web obtained from the modified direct strength method using compressive flat material properties;
$P^{\mathrm{T}}_{\mathrm{DSM}}$ = Nominal web crippling strength per web obtained from the proposed direct strength method using tensile flat material properties;
$P^{\mathrm{C}}_{\mathrm{EC3}}$ = Nominal web crippling strength per web obtained from European Code using compressive flat material properties;
$P^{\mathrm{T}}_{\mathrm{EC3}}$ = Nominal web crippling strength per web obtained from European Code using tensile flat material properties;
$P^{\mathrm{C}}_{\mathrm{EC3\#}}$ = Nominal web crippling strength per web obtained from European Code using actual bearing length and compressive material properties;
$P^{\mathrm{T}}_{\mathrm{EC3\#}}$ = Nominal web crippling strength per web obtained from European Code using actual bearing length and tensile flat material properties;
P_{Exp} = Experimental web crippling strength per web;
P_{FEA} = Web crippling strength per web obtained from finite element analysis;
$P_{\mathrm{NAS\#}}$ = Nominal web crippling strength per web obtained from modified North American Specification;
$P^{\mathrm{C}}_{\mathrm{NAS\#}}$ = Nominal web crippling strength per web obtained from modified North American Specification using compressive flat material properties;
$P^{\mathrm{T}}_{\mathrm{NAS\#}}$ = Nominal web crippling strength per web obtained from modified North American Specification using tensile flat material properties;
P_{cr} = Nominal bearing buckling strength per web;
P_{u} = Test and finite element strengths per web;
P_{y} = Nominal bearing yield strength per web;
R = Outer corner radius;
h = Depth of web flat portion;
r = Inner corner radius;
t = Web thickness;
β = Reliability index;
λ = Web crippling slenderness ratio;
$\sigma_{0.2}$ = 0.2% proof stress;
$\sigma^{\mathrm{C}}_{0.2}$ = 0.2% proof stress obtained from compressive flat coupon test;
$\sigma^{\mathrm{T}}_{0.2}$ = 0.2% proof stress obtained from tensile flat coupon test;
$\sigma_{0.2,\mathrm{c}}$ = 0.2% proof stress obtained from tensile corner coupon test; and
ϕ = Resistance factor.